

Effects of composition and microstructure on the abrasive wear performance of quenched wear resistant steels

Niko Ojala^{a,*}, Kati Valtonen^a, Vuokko Heino^a, Marke Kallio^b, Joonas Aaltonen^b, Pekka Siitonen^b and Veli-Tapani Kuokkala^a

^a Tampere Wear Center, Department of Materials Science, Tampere University of Technology, Tampere, Finland

^b Metso Minerals, Inc., Tampere, Finland

* Corresponding author: Niko Ojala; Tampere University of Technology, Department of Materials Science, P.O.Box 589, FI-33101 Tampere, Finland; tel. +358 50 317 4516; email niko.ojala@tut.fi

Abstract

Wear resistant steels are commonly categorized by their hardness, and in the case of quenched wear resistant steels, their Brinell hardness grades are widely considered almost as standards. In this study, the abrasive wear performance of 15 commercially available 400 HB grade quenched wear resistant steels from all over the world were tested with granite gravel in high stress conditions. The aim was to evaluate the real wear performance of nominally similar steels. Also properties such as hardness, hardness profiles, microstructures and chemical compositions of the steels were studied and reasons for the differences in their wear performance further discussed. In terms of mass loss, over 50 percent differences were recorded in the abrasive wear performance of the studied steels. Variations in the chemical compositions were linked to the auto-tempered microstructures of the steels, and the microstructural characteristics were further linked to their ultimate wear behavior.

Keywords: Wear testing; Abrasion; Steel; Mining, mineral processing; Hardness; Microstructure

1. Introduction

The commercial quenched wear resistant steels are commonly categorized by their Brinell hardness, e.g., as a 400HB grade or a 500HB grade steel. The hardness grades are considered almost as standards and as a guarantee of their wear performance. There is, however, a huge range of steels offered in each of the hardness categories, which makes a comparative study of nominally similar products worthwhile.

There are only few published studies related to the comparison of the actual wear performance of steels within the different hardness categories. Studies of the material properties, i.e. mainly hardness, which are affecting the wear performance of the steels, have been widely published [1, 2]. Also studies related to the product development concerning the optimization of the manufacturing process or the composition have been published [3, 4]. From the experience it is, however, evident that steels belonging to the same hardness category are not as similar regarding their wear resistance as they generally are thought to be. Results suggesting this have been published even before, and for example Moore [5] suggested already in 1974 that the microstructure of ferritic steels would have a greater influence than the bulk hardness when the wear resistance is considered. Rendón and Olsson [1] also found such indications in their study with three different microstructures.

The total cost of abrasive wear in industrial applications is estimated to be up to 4 % of the gross national product in the industrialized countries. In particular, the industrial applications handling loose soil, rocks or different minerals have to deal with the wear problems caused by abrasion [6]. Moreover, with the general progress of technology, also the capacities and production volumes are constantly growing, which means that the wear-related problems are not to diminish.

In this work, the abrasive wear properties of commercial 400 HB grade quenched wear resistant steels were tested to obtain a better understanding of the consistency of their wear performance. In total 15 different trade names from manufacturers all over the world were included in the study. The testing method simulated heavy abrasive wear in rock crushing and mineral processing, which are typical applications for the quenched wear resistant steels. Properties such as hardness, hardness profiles, microstructures and chemical compositions of commercial 400 HB grade quenched wear steels were studied and reasons for the differences in their wear performance are further discussed.

2. Materials and methods

Fifteen 400 HB grade quenched wear resistant steels were tested with the crushing pin-on-disk high stress abrasion wear tester [7] at the Tampere Wear Center. Fig. 1 illustrates the device, in which the gravel is cyclically pressed between a rotating disk and a sample pin. Table 1 presents the size distribution of the granite gravel, which was used as an abrasive.

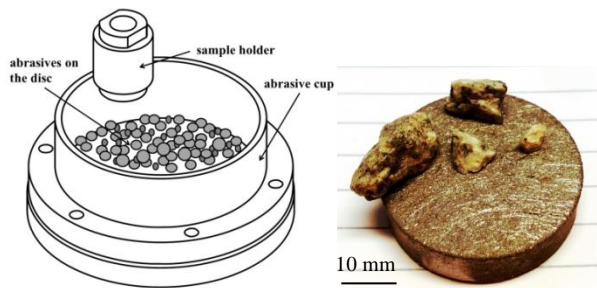


Fig. 1. Crushing pin-on-disk wear test device and a wear test sample with granite abrasives.

Table 1 Size distribution of the granite gravel used in the tests.

| Abrasive size [mm] | Mass fraction [g] |
|--------------------|-------------------|
| 8 / 10 | 50 |
| 6.3 / 8 | 150 |
| 4 / 6.3 | 250 |
| 2 / 4 | 50 |
| Total | 500 |

The test method is based on the pin-on-disk principle but without a direct pin-to-disk contact. The pin with a 36 mm diameter crushes the abrasive against the rotating disk. Each test in this study included a 15 minute pretest to reach steady-state wear, while the actual test duration was 30 minutes. The disk rotation speed was 20 rpm, and the pin was cyclically pressed down for 5 seconds and then lifted up for 2.5 seconds. In the current tests, 1.1 bar pin pressure was used, which gives a 235 N nominal crushing force. The disk material was S355 structural steel with a hardness of 200 HV. Three samples of each test material were tested. The wear rates were determined by weighing the samples five times during the tests.

Five of the fifteen wear tested steels were selected for a closer examination. The selection was based on the overall performance and initial surface hardness of the materials. Thus, steels with the lowest and highest mass losses and hardness values were selected.

The tested steels had a nominally similar alloying and the same microstructure and hardness, i.e., they were all quenched martensitic steels from the low-alloyed carbon steel group. Sheet thickness was 10 mm for steels A, B, C and E, and 12 mm for steel D. Table 2 presents the chemical compositions of the selected steels analyzed by optical emission spectrometer at Metso Minerals.

Table 2 Chemical compositions of the studied steels.

| Steel | A | B | C | D | E |
|----------------------------|-------|-------|-------|-------|-------|
| Chemical composition (wt%) | | | | | |
| C | 0.16 | 0.15 | 0.15 | 0.18 | 0.14 |
| Si | 0.4 | 0.28 | 0.22 | 0.2 | 0.38 |
| Mn | 1.38 | 0.96 | 1.35 | 1.38 | 1.41 |
| P | 0.015 | 0.012 | 0.007 | 0.015 | 0.014 |
| S | 0.002 | 0.003 | 0.002 | 0.003 | 0.001 |
| Cu | 0.01 | 0.02 | 0.05 | 0.06 | 0.03 |
| Cr | 0.14 | 0.37 | 0.41 | 0.18 | 0.46 |
| Ni | 0.04 | 0.07 | 0.09 | 0.06 | 0.04 |
| Mo | 0.15 | 0.1 | 0.01 | 0.19 | 0 |
| Al | 0.034 | 0.031 | 0.1 | 0.04 | 0.025 |
| N | 0.005 | 0.006 | 0.005 | 0.009 | 0.007 |
| V | 0.01 | 0.01 | 0.004 | 0.01 | 0.01 |
| B | 0.003 | 0.001 | 0.002 | 0.001 | 0.002 |
| Ti | 0.042 | 0.021 | 0.005 | 0.022 | 0.014 |

Before the tests, one millimeter was machined off from the sample surfaces to get rid of the decarburized layer. The surface hardness was measured from six points over the test surface. The hardness measurements were done in Vickers scale, where 420 HV corresponds to 400 HB. Moreover, the hardness profiles of the cross-sections were measured from the untested and tested samples. The microstructures of the steels, the wear surfaces and the wear surface cross-sections were characterized by optical and scanning electron microscopy (SEM). Nital was used for etching.

3. Results

Between the nominally similar 400 HB steels some substantial wear performance differences were observed. For example, the variation in the initial surface hardness values was more than 25 %, and in the wear tests the differences in the mass losses were as high as 53 %. On the other hand, the mass loss of the hardest steel was not the lowest, and the steel with the lowest hardness did not have the worst abrasive wear performance.

Fig. 2 presents the wear test results and the surface hardness values as averages of three tested samples. The standard deviations of the measured hardness values were small, 5-10 HV only. The results clearly indicate that the surface hardness differences do not explain the variations in the mass losses.

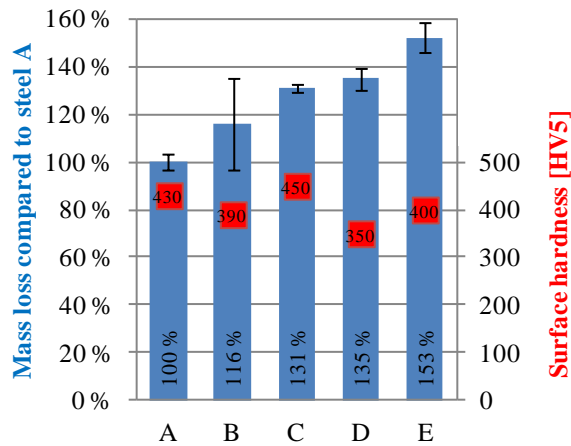


Fig. 2. Wear test results with standard deviation and initial surface hardness values. Average mass loss for steel A was 0.142 g.

3.1. Wear surfaces

After the wear tests, the wear surfaces were studied with optical and scanning electron microscopy. Fig. 3 presents the wear surfaces of steels A and E. In general, the steels with higher wear rates contained more scratches, which also were longer and deeper. The only exception was steel D, which did not have any deep cutting marks and was also less scratched than steel C. The selected test setup with a rather soft steel disc compared to the tested steel pins promotes two-body abrasion, as the abrasive particles tend to stick to the softer counter body and scratch the actual sample (pin) [8]. However, as also all pins had plenty of embedded granite on the surface, the overall wear mode appeared to be mixed two- and three-body abrasion.

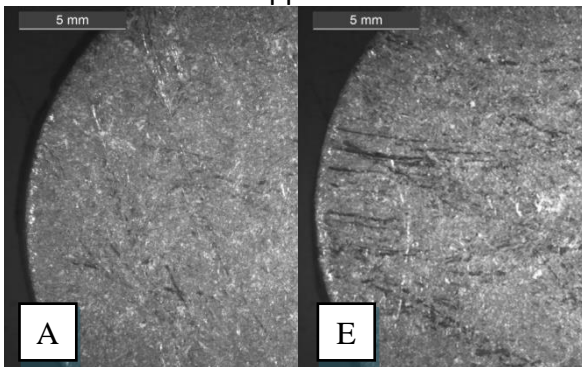


Fig. 3. Stereo microscope images of two wear surfaces.

For steel B, which showed the biggest scatter in the mass loss, all three wear surfaces were a little bit different in terms of surface scratching. In the most worn sample, long scratches were found all around the surface, while in the least worn sample only about a quarter of the wear surface contained such clearly visible scratches.

The SEM study showed that the scratches in steel A were fairly shallow, whereas in steel E the scratches were generally more distinct and deeper. Fig. 4 shows an example of a two-body abrasion wear scar with tear marks at the bottom of the scratch. These tear marks are formed by the tensile stress when the tip of the abrasive particle has slid over the surface.

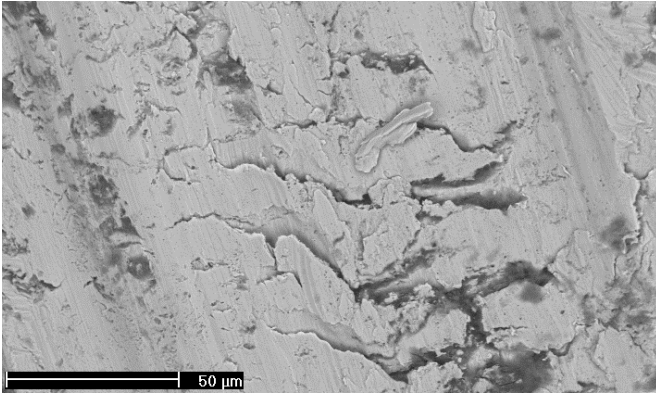


Fig. 4. SEM image of a steel B wear surface showing tear marks at the bottom of a scratch.

Fig. 5 shows a typical lip formation in steel E. No notable lip formation was observed in steels A and B. The lips were mainly formed over the embedded abrasive particles or hard surface layers by the subsequent plastic deformation over the same area. These kinds of lips are prone to become loose as they normally are not well attached to the surface beneath. High formation frequency of such lips may result in a higher wear rate.

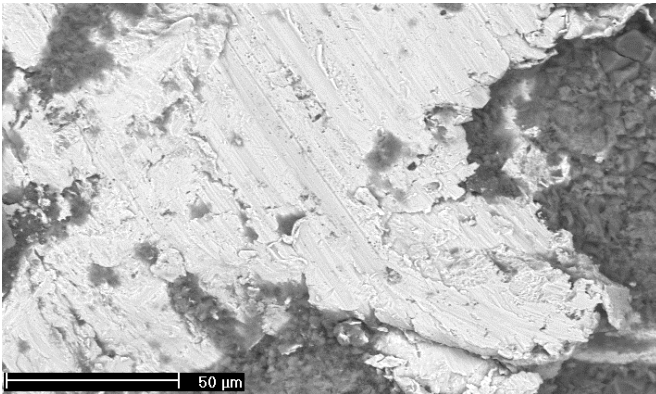


Fig. 5. SEM image of a steel E wear surface showing the end of a wide scratch mark and a lip formed over an embedded granite particle.

The roughness of the wear surfaces were analyzed with an optical profilometer. Both R_a and R_q values were determined because they are different measures of the surface profile. The R_a value, i.e., the average of the absolute values, is the most commonly used, but it may not describe the wear surfaces in the best possible manner. Instead, the R_q value, i.e., the root mean square value of the surface profile, is more sensitive to the high peaks and low valleys typical to a wear surface.

Fig. 6 presents the measured R_a and R_q values in an ascending order together with the initial surface hardness values for all studied steels. Both the R_a and R_q values arrange in an increasing order with the decreasing average surface hardness values measured before the wear test. Thus, softer surface results in higher surface roughness, as could be expected.

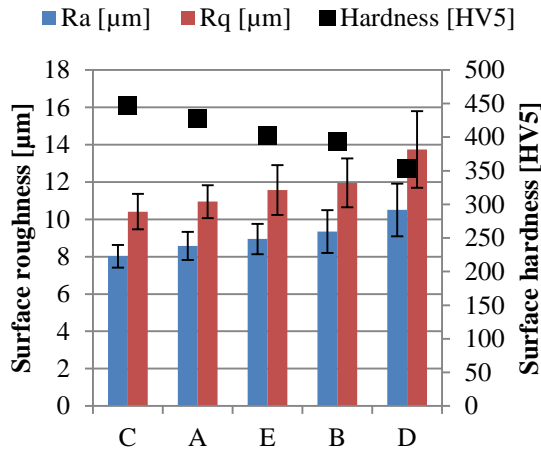


Fig. 6. Average Ra and Rq values for the tested steels arranged in the order of the average initial surface hardness values.

3.2. Hardness profiles

The hardness profiles of the steels shown in Fig. 7 were measured from untested samples. The hardness profiles after removal of the decarburized layer were fairly stable, especially close to the surface where the variations were around 10 HV for all samples. It was, however, observed that after an initially stable start the hardness profile of steel D was fluctuating between 375 and 460 HV. For checking, also the through plate hardness profile of steel D was measured and found to vary throughout the thickness, which may indicate problems in the manufacturing process, either the rolling or heat treatment, of this steel.

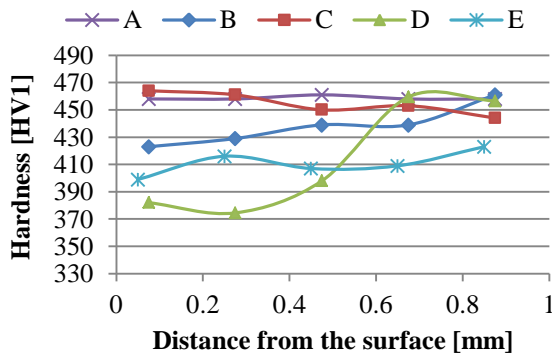


Fig. 7. Hardness profiles determined from the untested samples.

3.3. Chemical compositions

The chemical compositions presented in Table 2 were used to calculate the total amount of alloying elements, the martensite start (M_s) temperatures and carbon equivalent (C_{eq}) values for the studied materials. These values are important as the outcome of the quenching process can be predicted and analyzed based on them. For example, the higher the M_s temperature, the more time and energy there is for auto-tempering to happen [9]. Also, the lower the CE value, the more ductile the forming microstructure will be [10].

The results of the calculations are shown in Table 3. The M_s temperatures were calculated using two different formulas. The first one was published by Ishida [11] in 1995, and the second one is the widely used formula published by Steven and Hayes [12] in 1956. Both formulas show small but clear differences between the studied steels, giving the highest value for steel B and the lowest

value for steel D.

Also the carbon equivalent values were calculated using two different formulas. The first one, denoted as “C_{eq}”, is the widely used IIW-formula, and the other one, denoted as “Pcm”, is the so-called critical metal parameter formula developed by The Japanese Welding Engineering Society for weld cracking [13]. Again the differences are small, steel B showing the best (smallest) and steel D the worst (highest) value.

Table 3 Total amounts of the alloying elements with calculated M_s temperatures and carbon equivalents.

| Steel | A | B | C | D | E |
|--|------|------|------|------|------|
| Total amount of alloying elements (wt%) | | | | | |
| | 2.42 | 2.05 | 2.46 | 2.36 | 2.54 |
| Martensite start temperature (°C) | | | | | |
| M _s ^a | 454 | 465 | 455 | 448 | 456 |
| M _s ^b | 433 | 449 | 437 | 422 | 440 |
| Carbon equivalent | | | | | |
| C _{eq} ^c | 0.45 | 0.41 | 0.47 | 0.49 | 0.47 |
| Pcm ^d | 0.28 | 0.24 | 0.26 | 0.29 | 0.26 |

$$^a M_s(^{\circ}\text{C}, \text{wt}\%) = 545 - 330\text{C} + 2\text{Al} + 7\text{Co} - 14\text{Cr} - 13\text{Cu}$$

$$- 23\text{Mn} - 5\text{Mo} - 4\text{Nb} - 13\text{Ni} - 7\text{Si} + 3\text{Ti} + 4\text{V} + 0\text{W}$$

$$^b M_s(^{\circ}\text{C}, \text{wt}\%) = 561 - 474\text{C} - 17\text{Cr} - 33\text{Mn} - 21\text{Mo} - 17\text{Ni}$$

$$^c C_{eq} = \text{C} + \text{Mn}/6 + (\text{Cr} + \text{Mo} + \text{V})/5 + (\text{Cu} + \text{Ni})/15$$

$$^d \text{Pcm} = \text{C} + \text{Si}/30 + (\text{Mn} + \text{Cu} + \text{Cr})/20 + \text{Ni}/60 + \text{Mo}/15$$

$$+ \text{V}/10 + 5\text{B}$$

3.4. Microstructures

Fig. 8 presents optical micrographs of the steels taken from the cross sections of untested samples. The micrographs show that all steels have a tempered martensite microstructure, the lath structure of which was well visible in the optical microscope. The unetched white grains seen in the micrographs are untempered white martensite, which is a hard and brittle phase. The grain sizes and fractions of the white martensite shown in Table 4 were manually measured with image analysis software.

Although it is difficult to delineate the parent austenite from the Nital etched microstructures, steels B, D and E evidently have the largest parent austenite grain sizes. General differences, however, can be easily seen between the steels, for example that steel A has the most homogenous microstructure and that steel B contains the finest white martensite structure. The steels with the highest hardness values, i.e., A and C, have the shortest martensite laths, which also appear rather thick.

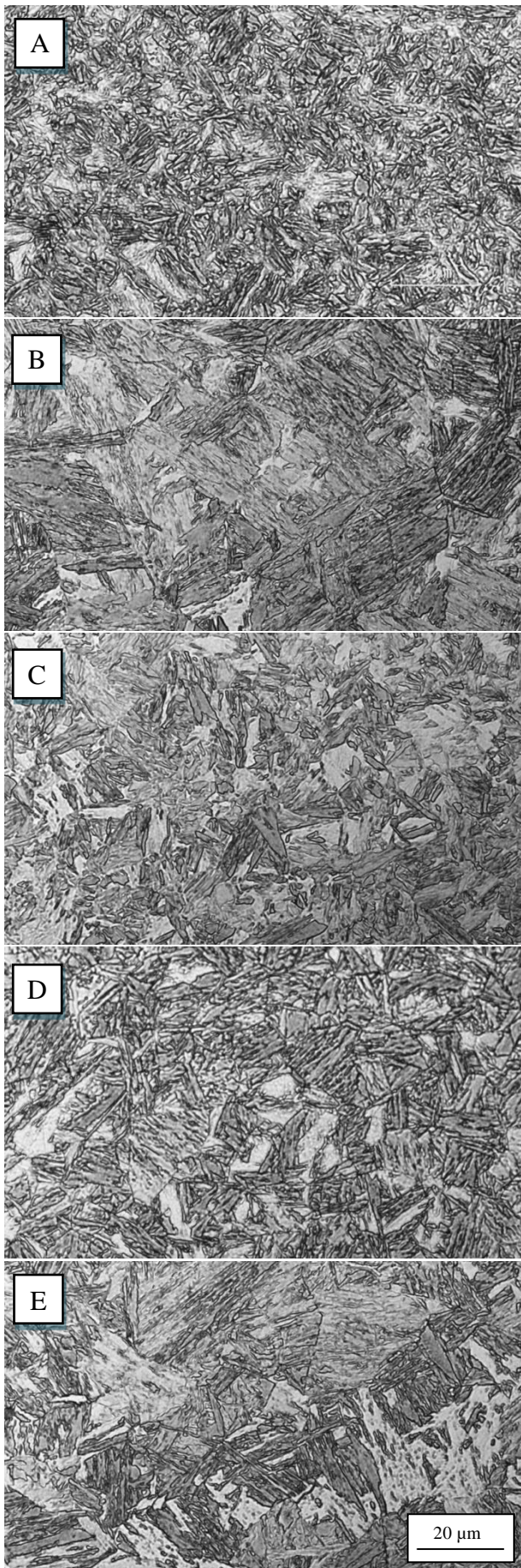


Fig. 8. Optical micrographs of the studied steels.

Table 4 White martensite contents and grain size measurements.

| Steel | A | B | C | D | E |
|--------------------------------------|----|----|----|----|----|
| White martensite | | | | | |
| % | 17 | 20 | 31 | 29 | 29 |
| avg. μm | 3 | 2 | 5 | 4 | 3 |
| max ^a μm | 5 | 7 | 8 | 9 | 12 |
| Parent austenite / Grain size | | | | | |
| avg. μm | 14 | 22 | 16 | 19 | 27 |

^a average of the largest white martensite grains

3.5. Wear surface cross-sections

The surface deformations, changes in the microstructures, and microhardness values were determined from the wear surface cross-sections. For all steels, the surface layers were heavily deformed and the martensite laths were mechanically fibered. The thickness of the visibly deformed layer varied from some micrometers to about 60 μm . To further evaluate the extent of work hardening, microhardness profiles were measured using a load of 50 grams. After 60 to 100 μm , the hardness profiles start to stabilize. On average, steel B showed clearly strongest work hardening, while the rest of the steels arranged in the order of the wear test results. Steel C still remained the hardest.

The clearest difference in the deformation behavior of the studied steels was in their ability to deform plastically and in the average thickness of the deformed layer. Fig. 9 presents the wear surface cross-sections of the steels. Steels A and B were more evenly deformed than the others, and they also showed the highest overall plastic flow. Moreover, the deformation zone was clearly visible with a smooth transition to the base material. The other steels contained mostly very thin surface layers with a sharp interface with the base material. Those layers had very fine microstructures and high hardness. The hardest layer in steel B was 605 HV0.05, while in steel C it was 820 HV0.05. Steels C, D, and E had much thinner deformation zones than A and B, and they also showed plenty of rather brittle chip formation. Cracked or partially detached surface layers were observed almost in all plastically deformed areas on the surfaces of steels C, D and E.

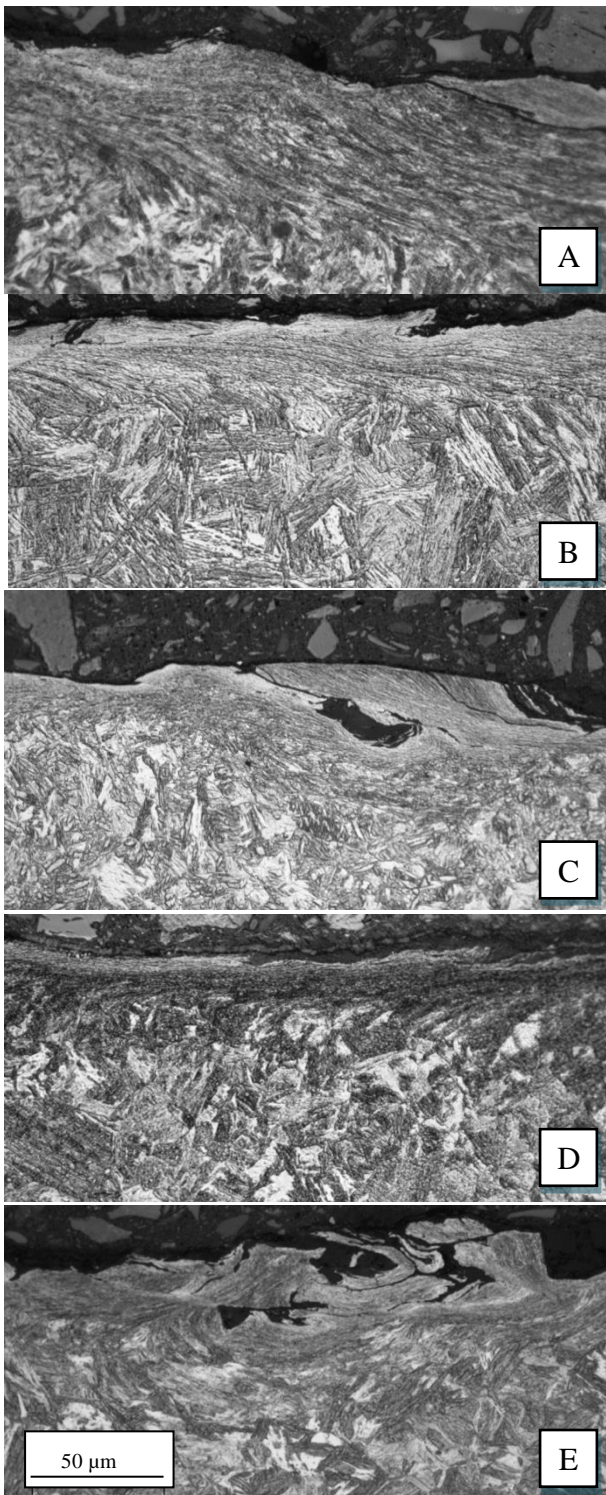


Fig. 9. Optical micrographs of the wear surface cross-sections.

In addition to the optical micrographs presented in Fig. 9, the SEM image in Fig. 10 shows in more detail the thin and brittle surface deformation zone in steel C. This tribolayer has formed from crushed granite and steel, and in most cases it was cracked or already partially detached. The average thickness of the layer was only a few micrometers, but as seen in Fig. 10, there were also thicker sections. These may have formed during the embedment of larger abrasive particles. In general, a thicker layer is more brittle and more prone to crack formation and eventual spalling.

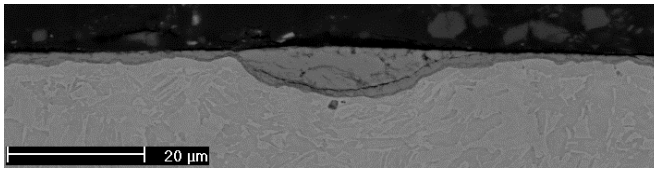


Fig. 10. Cross-sectional SEM image of steel C, showing a granite-steel tribolayer with a thicker section, which is detaching from the surface.

Fig. 11 presents a SEM image of the wear surface of steel B, revealing the evidently more ductile behavior of this steel compared to steel C. The brittle tribolayer formed on the surface of steel C was not observed on the surface of steel B, which also had the clear and smooth deformation zone already noticed in the optical micrographs.

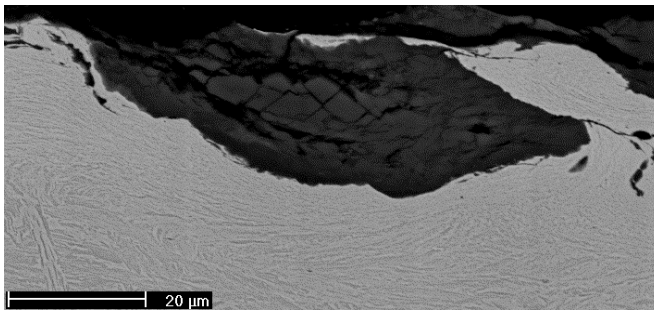


Fig. 11. Cross-sectional SEM image of steel B, showing an embedded granite particle and revealing the absence of the tribolayer and the high deformation capability of the steel.

4. Discussion

This study has revealed significant differences in the heavy abrasive wear performance of nominally similar 400 HB grade quenched wear resistant steels. The wear rate of steel A, which had a 430 HV (~ 410 HB) surface hardness, was 31 % lower than that of the 450 HV steel C, and even 53% lower than that of the 400 HV steel E. Consequently, if a wear resistant steel is changed to another nominally similar steel (with the same HB grade), the risk of unexpected failure of the wear part is evident.

Noticeable differences between steels belonging to the same hardness category or grade could be observed in the chemical compositions and microstructures as well as in the mechanical behavior on the wear surface. Although it has become evident that the surface hardness or the hardness profile are not sufficient factors to explain the wear test results, a closer examination of both of these factors can offer some explanations.

4.1. Chemical composition and microstructure

The wear performance of quenched steels usually depends on the concentration of their main alloying elements, i.e., carbon, molybdenum and boron. These elements are important for the quenched wear resistant steels, as they either raise the hardness, like carbon, or more importantly enhance the hardenability of the steel, like molybdenum and boron [14]. Moreover, the combined concentration of nickel and molybdenum also affects the wear performance. Steel D had the highest carbon and molybdenum content of the studied steels, but the strongly fluctuating hardness profile points to some manufacturing problems. Therefore steel D will be omitted in the further discussion.

Steel A had the highest boron and combined nickel-molybdenum contents and the lowest wear

rate. Nickel-molybdenum as a combination has a larger effect on the hardenability of the steel than either one of the elements alone. In low-carbon steels, boron has the biggest effect on the hardenability as a single alloying element, even in small quantities. Boron promotes the martensitic transformation by delaying the ferrite-pearlite transformation. [14, 15] However, boron needs to be protected from oxygen and nitrogen by deoxidizing and addition of strong nitride formers such as aluminum and titanium, as otherwise it will react with nitrogen and the hardenability effect is lost [16].

Steel E with the worst wear performance contained the least amount of boron protectors and not at all molybdenum, and obviously therefore exhibited the poorest hardenability of the studied steels. The large amount of white martensite in its microstructure supports this conclusion.

Steels A and C had similar hardness, but the grain size of steel C was larger and it also contained more of the brittle white martensite. The reason for this can be the aluminum and silicon content, as steel C contained substantially more aluminum and at the same time the least amount of silicon compared with the other studied steels. Aluminum and also nickel have been reported to increase the stacking fault energy of austenite and thereby to hinder the martensite formation. Silicon, on the other hand, decreases the stacking fault energy. [17] For martensitic wear resistant steels the amount of white martensite over tempered martensite is crucial, because white untempered martensite is very brittle.

Furthermore, there were also some differences in the total amounts of the alloying elements. Generally all alloying elements either decrease the M_s -temperature or restrain the decomposition of austenite, both resulting in the retardation of martensite formation [14]. Steel B, which had the finest white martensite grains, had clearly the smallest amount of alloying elements, in total 2.05 wt%, while steel E had the highest amount of 2.54 wt%. Steels B and E had almost the same bulk hardness, but the difference in their wear performance was notable, obviously due to the large difference in their alloying.

Features of the martensitic transformation, such as the M_s -temperature and austenite decomposition rate, are of great importance in obtaining the best possible material characteristics for a wear resistant steel. As the tested steels are manufactured without tempering, the role of auto-temperability cannot be ignored. It dictates the amount of tempered martensite during the manufacturing, and hence the ductility of the resulting microstructure [9]. The higher the M_s -temperature and the austenite decomposition rate are, the more time there is for tempered martensite to form.

As a summary of the role of the chemical composition, the wear resistant steels need a sufficient amount of carbon and boron and a high combined nickel-molybdenum level to show the required hardenability. Moreover, sufficient ductility is also needed from the steels used in abrasive conditions. The required properties can be obtained by good auto-temperability and proper manufacturing methods that produce a homogenous martensitic microstructure with low amounts of fine grained white martensite, like in steels A and B.

4.2. Surface deformation and work hardening

In abrasive wear conditions, the common engineering surface roughness values, R_a and R_q , depend inversely on the average surface hardness measured before the wear testing. Similar results related to impact-abrasion wear have also been presented [18].

In the worn samples studied in this work, the deformation depth visible in optical microscopy was low, at highest only about 60 μm . It is, however, evident that also the actual microstructure of the deformation zone below the surface affects the abrasive wear caused by large granite particles of up to 10 mm in size. Misra and Finnie [19] reported for soft steels that particles larger than the thickness of the hardened layer can penetrate it and thereby decrease or completely eliminate the effect of work hardening. However, when the deformation zone offers a smooth transition from the work hardened surface, it will require more energy for large particles to penetrate the surface layer and remove material from the sample.

The surface structures were mechanically fibered in all steels, but clear differences in the degree of fibering and the amount of deformation could be observed. Mechanical fibering, and the anisotropic properties it creates, are often ignored with engineering steels. However, in abrasive wear, the stresses are more or less perpendicular to the fibering direction, i.e., perpendicular to the surface, which according to Hosford [20] may lead to delamination. From the tested steels, two groups can be distinguished. On average, steels A and B had a thicker and smoother deformation zone than the rest of the test materials, which explains why cracks, inclusions and delamination in the deformed surface areas were observed only in steels C, D and E. This kind of brittle behavior arises from the insufficient ability of the material to deform plastically.

Hardell et al. [21] reported that different quenching methods for the same boron steel resulted in very different hardness values but still comparable wear performance in unidirectional abrasive wear. They concluded that this was due to the work hardening of the surface layer. In the current work, steel B, the initially second softest steel, work hardened most and was ranked second in the wear performance. On the other hand, steel E, which showed the poorest hardenability also work hardened least and was ranked last in the wear performance.

It appears that in heavy abrasive wear the surface needs the ability to withstand multidirectional and repeated deformations. Steels A and B performed exceptionally well in such conditions. In contrast to this, in steels C, D and E the intense plastic deformation led to a highly work hardened thin surface layer and/or formation of a tribolayer. Both of these will increase the surface hardness, but such hard surface layers can increase the wear resistance only if the subsurface layers can support them sufficiently. Heino et al. [22] found that the same kind of hard surface layers will easily peel off from steels with hardness similar to those studied in this work. If the thin surface layers peels off, the wear loss will increase accordingly.

As a summary, the initial surface hardness is not so decisive when the abrasive wear causes marked plastic deformation on the surface of the material. At least equally important is the steel's ability to retain its ductility during abrasive wear, in particular in rock crushing and other highly abrasive mineral processing applications. This was especially evident when steels B and C were compared with each other.

5. Conclusions

The initial motivation for this study was quite practical, i.e., to reveal the possible differences in the wear performance of nominally similar 400 HB grade quenched wear resistant steels commonly used by industry in various wear related applications. In the study, the abrasive wear performance was experimentally determined for 15 different commercially available 400 HB grade steels, five of which were then selected for a closer examination. As abrasive wear covers about two thirds of the industrial wear problems, this kind of a comparative study is of significant practical importance for

the steel producing and using industries. The results of this work can be utilized, for example, in various mineral handling applications, such as crushing and transportation of minerals.

The main observation was that the nominally similar 400 HB grade quenched wear resistant steels do not perform equally under heavy abrasive wear, and hardness alone is not an accurate predictor of the steel's wear performance. Alloying and manufacturing of the steel and thus its microstructure and hardness profile have a significant effect particularly on the work hardening and mechanical behavior of the steel during abrasion, leading to different wear performances under such conditions.

Good abrasive wear performance in applications dealing with natural minerals requires certain hardness, but also sufficient ductility of the contact surface is needed, even after substantial work hardening. If the surface becomes too brittle, the wear rate increases rapidly. Furthermore, in the cases when the deformation zone does not offer smooth transition between the wear surface and the base material, the wear rates tend to become higher. Based on the results of this work, the abrasive wear life of nominally similar 400 HB grade quenched wear resistant steels can vary markedly, which should be taken into account in the materials selection processes.

Acknowledgements

The work has been done within the FIMECC DEMAPP program funded by Tekes and the participating companies. The corresponding author would like to express his gratitude to Jenny and Antti Wihuri Foundation.

References

- [1] J. Rendón and M. Olsson, Abrasive wear resistance of some commercial abrasion resistant steels evaluated by laboratory test methods, *Wear* 267 (2009) 2055-2061.
- [2] V. Ratia, K. Valtonen, A. Kemppainen and V.-T. Kuokkala, High-Stress Abrasion and Impact-Abrasion Testing of Wear Resistant Steels, *Tribology Online*, 8, 2 (2013) 152-161.
- [3] A.K. Jha, B.K. Prasad, O.P. Modi, S. Das and A.H. Yegneswaran, Correlating microstructural features and mechanical properties with abrasion resistance of a high strength low alloy steel, *Wear* 254 (2003) 120-128.
- [4] X. Deng, Z. Wang, Y. Han, H. Zhao and G. Wang, Microstructure and Abrasive Wear Behavior of Medium Carbon Low Alloy Martensitic Abrasion Resistant Steel, *Journal of Iron and Steel Research, International*, 2014, 21(1), p 98-103.
- [5] M.A. Moore, The relationship between the abrasive wear resistance, hardness and microstructure of ferritic materials, *Wear* 28 (1974) 59-68.
- [6] J.H. Tylczak, *Abrasive Wear, Friction, Lubrication, and Wear Technology*, Vol 18, ASM Handbook, ASM International, 1992, p 184-190.
- [7] J. Terva, T. Teeri, V.-T. Kuokkala, P. Siitonen and J. Liimatainen, Abrasive wear of steel against gravel with different rock-steel combinations, *Wear* 267 (2009) 1821-1831.
- [8] N. Axén, S. Jacobson and S. Hogmark, Influence of hardness of the counterbody in three-body abrasive wear — an overlooked hardness effect, *Tribology International*, vol 27, issue 4, August 1994, p 233-241.
- [9] H. Matsuda, R. Mizuno, Y. Funakawa, K. Seto, S. Matsuoka, Y. Tanaka, Effects of auto-tempering behaviour of martensite on mechanical properties of ultra high strength steel sheets, *Journal of Alloys and Compounds* 577S (2013) S661–S667.
- [10] H. Sunga, S. Shina, B. Hwangb, C. Leeb, N. Kimc and S. Lee, Effects of carbon equivalent and cooling rate on tensile and Charpy impact properties of high-strength bainitic steels, *Materials Science and Engineering A* 530 (2011) 530–538.

- [11] K. Ishida, Calculation of the effect of alloying elements on the M_s temperature in steels, *Journal of Alloys and Compounds* 220 (1995) 126-131.
- [12] W. Steven and A.G. Haynes: The temperature of forming martensite and bainite in low-alloy steels. *Journal of the Iron and Steel Institute*, 183, 349-359 (1956).
- [13] J.F. Lancaster, *Metallurgy of welding* (6th edition), Abington Publishing, p. 464, 1999, ISBN 978-1-85573-428-9.
- [14] G. Krauss, *Microstructures and Properties of Carburized Steels, Heat Treating, Vol 4*, ASM Handbook, ASM International, 1991, p 363-375.
- [15] J. Tungtrongpairoj, V. Uthaisangsuk and W. Bleck, Determination of Yield Behaviour of Boron Alloy Steel at High Temperature, *Journal of Metals, Materials and Minerals*, vol 19, no.1, 2009, p 29-38.
- [16] G. Haywood, Boron in Steel, *Steeluniversity.org*, World Steel Association, 2012.
- [17] S. S. F. Dafé, D. R. Moreira, M. S. Matoso, B. M. Gonzalez and D. B. Santos, Martensite Formation and Recrystallization Behavior in 17Mn0.06C2Si3Al1Ni TRIP/TWIP Steel after Hot and Cold Rolling, *Materials Science Forum*, vol. 753, 2013, p 185-190.
- [18] V. Ratia, I. Miettunen and V.-T. Kuokkala, Surface deformation of steels in impact-abrasion: The effect of sample angle and test duration, *Wear* 301 (2013) 94-101.
- [19] A. Misra and I. Finnie, On the size effect in abrasive and erosive wear, *Wear* 65 (1981) 359-373.
- [20] W. F. Hosford, *Mechanical Behavior of Materials*, Cambridge University Press, 2010, USA.
- [21] J. Hardell, A. Yousfi, M. Lund, L. Pelcastre and B. Prakash, Abrasive wear behaviour of hardened high strength boron steel, *Tribology – Materials, Surfaces & Interfaces*, 8(2) (2014) 90-97.
- [22] V. Heino, K. Valtonen, P. Kivikytö-Reponen, P. Siitonen and V.-T. Kuokkala, Characterization of the effects of embedded quartz layer on wear rates in abrasive wear, *Wear* 308 (2013) 174-179.